

Supporting Information

A nanohybrids coupling of NiPS₃ nanoparticles and defective graphene as a pH-universal electrocatalysts for efficient water splitting

Jian Zhang, Renjie Cui, Xing'ao Li*, Xiaoheng Liu, Wei Huang*

*Corresponding Author: lxahbmy@126.com

*Corresponding Author: iamwhuang@njupt.edu.cn

Experimental Section

Preparation of precursor $\text{Ni}_2(\text{CO}_3)(\text{OH})_2$.

The uniform $\text{Ni}_2(\text{CO}_3)(\text{OH})_2$ nanoparticles were synthesized by a mild hydrothermal process. All chemicals in this work are of analytical purity and used without further purification. In short, 1.5 g of nickel nitrate hexahydrate ($\text{Ni}(\text{NO}_3)_2 \cdot 6\text{H}_2\text{O}$, 98%, Sigma-Aldrich) was dissolved in 35 mL of distilled water to form a clear solution by magnetic stirring. After that, 0.08 g of urea ($\text{CO}(\text{NH}_2)_2$, AR, Shanghai Chemical Factory of China) and 0.05 g poly(vinylpyrrolidone) (PVP, AR, Shanghai Chemical Factory of China) were added successively. After magnetic stirring over 30 min, the mixture solution was transferred to a 50 mL Teflon-lined stainless autoclave and heated at 130 °C for 12 h. After cooling to room temperature naturally, the precipitate was collected by centrifugation and washed with distilled water and absolute ethanol two times each and dried in a vacuum oven at 50 °C (12 h). The dark green powder was collected and dried in a vacuum oven at 60 °C (12 h).

Preparation of NiPS_3 .

NiPS_3 nanoparticles was synthesized by an one-step sulfue-phosphidation methods.[2]

The obtained $\text{Ni}_2(\text{CO}_3)(\text{OH})_2$ precursor were put at the downstream end of the tube, outside the heating area of the furnace, and a mixture (1:1) of sulphur (Sigma-Aldrich, 99.5 %) and phosphorus (Sigma-Aldrich, 99.0%) powders at the upstream side of the furnace. The furnace was first heated to 200 °C within 20 min and maintained 15 min under Ar carrier gas (99.999%) at 50 sccm. After cooling to room temperature

naturally, the alumina boat with a thiophosphate (P_xS_y) paste-like product from the mixture sulphur and phosphorus was moved to the upstream edge of the furnace, and the precursor vessel ($Ni_2(CO_3)(OH)_2$) was moved to the heating zone of the furnace. The furnace was then heated to 500 °C for 1 h to convert these precursors to $NiPS_3$ before the furnace was cooled down naturally.

Preparation of defective graphene (DG).

DG was synthesized by high temperature annealing method. Typically, the monolayer graphene was mixed with melamine (mass ration is 1:1), and annealed at 700 °C for 2 hours under nitrogen. Then, the above powder was annealed at 1150 °C for 2 hours with a ramp rate of 5 °C min^{-1} under an atmosphere of nitrogen to produce the topological defects on the surface and edge of the graphene.

Preparation of $NiPS_3@DG$ nanocomposites.

In detail, a designed volume of G and DG nanosheet (0.2 g L^{-1}) was added drop by drop into the $NiPS_3$ nanoparticles suspension under continuous stirring. The flocculated product was separated by centrifugation.

Materials characterizations.

The morphologies of the samples were characterized by transmission electron microscopy (TEM) (FEI Tecnai F20) at an acceleration voltage of 200 kV. Scanning transmission electron microscopy (STEM) was performed using a FEI Titan 80-200

(ChemiSTEM) electron microscope operated at 200 kV, equipped with a high angle annular dark field (HAADF) detector, while compositional maps were obtained with energy dispersive spectroscopy (EDS) using four large solid-angle symmetrical Si drift detectors. Scanning electron microscopy (SEM) was taken on a Hitachi S-4800 scanning electron microscope. X-ray photoelectron spectra (XPS) were acquired on an ESCALAB MK II with Mg K α as the excitation source. Atomic force microscopy (AFM) on a Veeco Multimode using the tapping mode. The BET surface area was measured using the nitrogen gas adsorption-desorption method (TriStar II 3020) at 77 K. XRD measurements were carried out on a BRUKER D8 Advance X-diffractometer with Cu K α radiation. Raman spectra were recorded on a Raman spectroscopy was performed with a laser micro-Raman spectrometer (Renishaw in Via, 532 nm excitation wavelength). Inductively coupled plasma atomic emission spectrometry (ICP-AES) analysis was performed on a Thermo ICAP-6300 instrument (USA).

Density functional theory (DFT) calculations.

The projected augmented wave (PAW) scheme as incorporated in the Vienna ab initio simulation package (VASP) was used in the study.[1-3] The Monkhorst and Pack scheme of k point sampling was used for integration over the first Brillouin zone [4] and accounting for spin polarisation. The hydrogen adsorption energies were computed with slabs of 1 x 3 x 1 grid. A sufficiently large slab was used so that the monolayers in the neighbouring cells in the vertical (z-axis) and horizontal directions (x-axis) were separated by 20 Å. The lattice parameters obtained were, a = b = 5.8208

\AA , $c = 6.627 \text{ \AA}$; $\alpha = \beta = 98.458$, $\gamma = 120.8$. A simple model of NiPS_3 slab consisting of 18 sulphur, 6 phosphorus and 6 nickel atoms was used. All the structures were relaxed to a tolerance of less than 0.1 eV\AA^{-1} . The associated free energy of chemisorption was calculated by correcting for both the zero-point vibrational energy and the loss of translation entropy of H_2 (g) on adsorption, and neglecting the smaller vibrational entropy terms. The zero-point contributions were considered (for NiPS_3) to be, $\Delta G = \Delta E + 0.24 \text{ eV}$. The hydrogen chemisorption energy (ΔE_{H}) was calculated using the following equation:

$$\Delta E_{\text{H}} = E(\text{NiPS}_3 + n\text{H}) - E(\text{NiPS}_3 + (n-1)\text{H}) - n/2E(\text{H}_2)$$

where $E(\text{NiPS}_3 + n\text{H})$ is the total energy of the NiPS_3 slab along with different hydrogen coverages, $E(\text{NiPS}_3 + (n-1)\text{H})$ is the total energy of NiPS_3 slab and $E(\text{H}_2)$ is the DFT energy for hydrogen molecule in the gas phase. Our modelled slab shows six different phosphorus sites and four Ni sites with four co-ordination; remaining two Ni sites are octahedrally coordinated.

Electrochemical characterization of catalytic activity towards the HER.

Electrochemical measurements were collected through a three-electrode system on an electrochemical workstation (Chenhua, CHI660E, Shanghai), using Ag/AgCl (saturated KCl solution) electrode as the reference electrodes, Pt mesh and glassy carbon rod as the counter electrodes and glassy carbon (GC) electrode as the working electrode. All the measurements were carried out in 30 mL of electrolyte (purged with H_2 for 30 min) : 0.5 M H_2SO_4 (pH 0.30), 1 M KOH (pH 14.00), and 1 M PBS (pH

7.00) (dissolve 13.61 g KH_2PO_4 in 100 mL deionized water, and the pH of the mixture was adjusted to 7.00 with 1 M KOH). 4 mg of catalyst powder and 30 μL Nafion solution (Sigma Aldrich, 5% wt) were dispersed in 2 mL water isopropanol solution with a volume ratio of 3 : 1 by sonicating for 1 h. Then, 20 μL (40 μg catalyst) of the dispersion was dripped onto a glassy carbon electrode as the working electrode. The electrochemical stability of the catalyst was evaluated (0.1 ~ -0.4 V vs. RHE) with a scan rate of 10 mV s^{-1} . The electrochemical impedance spectroscopy (EIS) was carried out in the range from 100 K to 0.01 Hz with an AC amplitude of 10 mV. All polarization curves were corrected for iR losses unless otherwise noted. To determine C_{dl} for each $\text{NiPS}_3@\text{DG}$ electrode, three CV cycles were recorded (100 ~ 200 mV vs. RHE) in the standard measurement configuration described above at scan rates of 4, 10, 20, 40, 60, 80, 100 and 120 mV s^{-1} . The two CV cycles at each scan rate were compared to ensure consistency, and the second cycle was always used for C_{dl} determination. Then, for each scan rate, ΔJ was measured at - 0.15 V vs. RHE and plotted against the scan rate. These data were then fit to a line, the slope of which is equal to twice the geometric C_{dl} . The turnover frequency (TOF) values and the active site numbers (n) can be confirmed according to the reported method [5] by a CV test in 1.0 M phosphate buffer solution (PBS, pH = 7) at a scan rate of 50 $\text{mV}\cdot\text{s}^{-1}$ from -0.2 to 0.6 V vs the RHE.

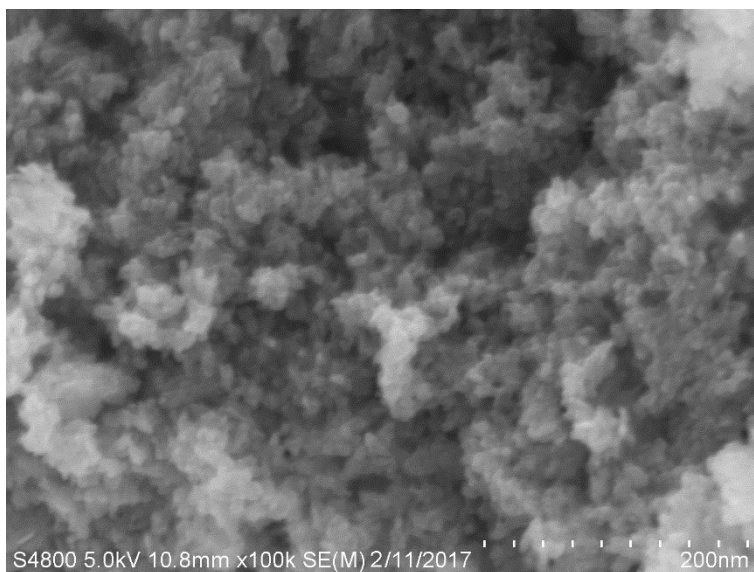


Fig. S1 SEM image of $\text{Ni}_2(\text{CO}_3)(\text{OH})_2$ precursor.

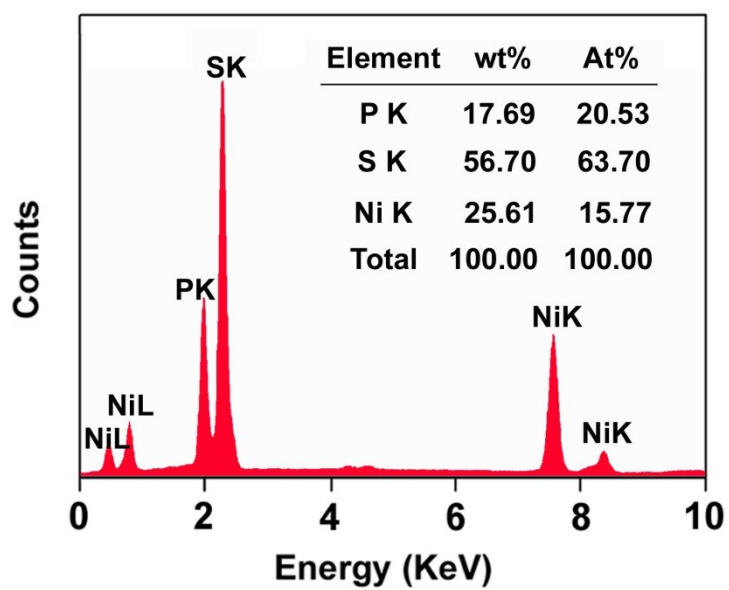


Fig. S2 Energy-X-ray spectra of NiPS_3 .

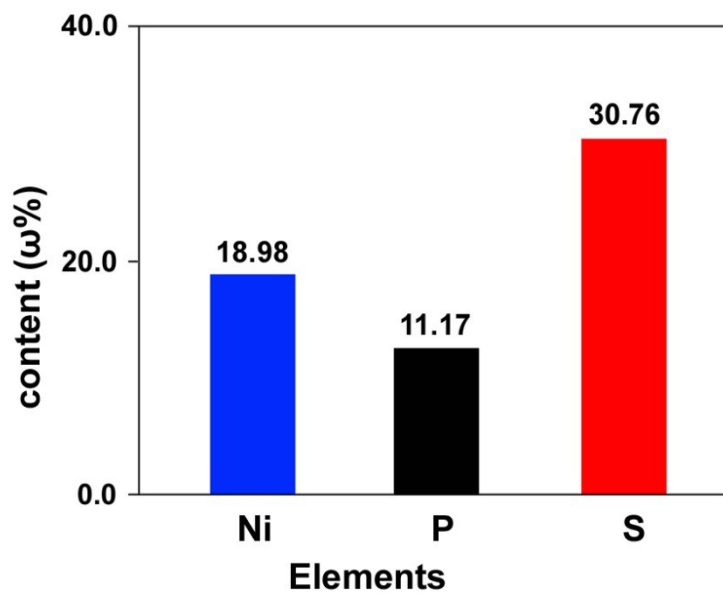


Fig. S3 ICP analysis results of the as-synthesized NiPS₃@DG.

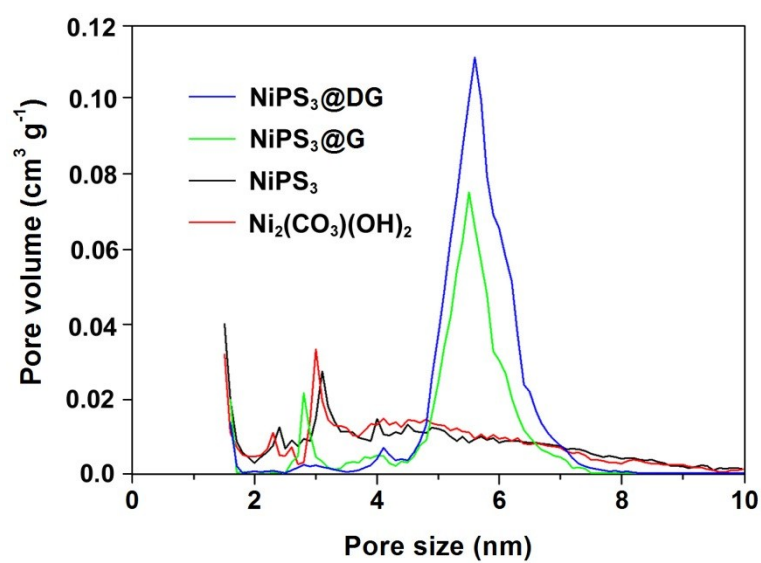


Fig. S4 Pore-size distribution curves of Ni₂(CO₃)(OH)₂, NiSP₃, NiSP₃@G, and NiSP₃@DG.

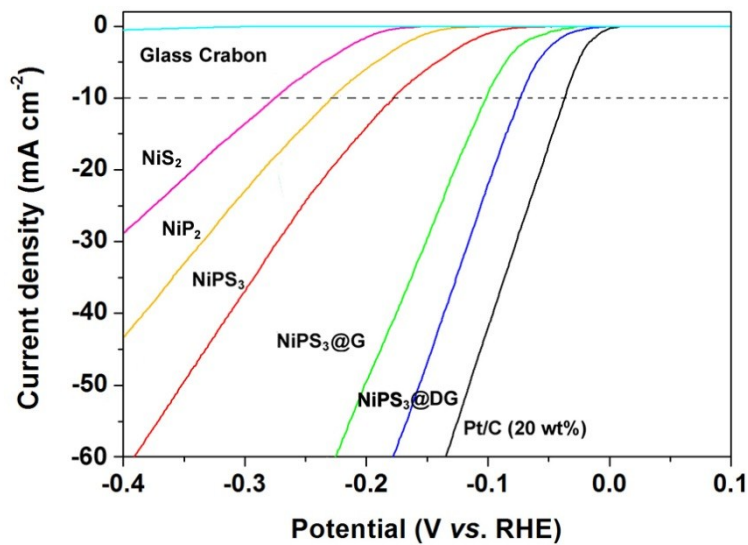


Fig. S5 The comparison experiments among various sulfide based catalyst.

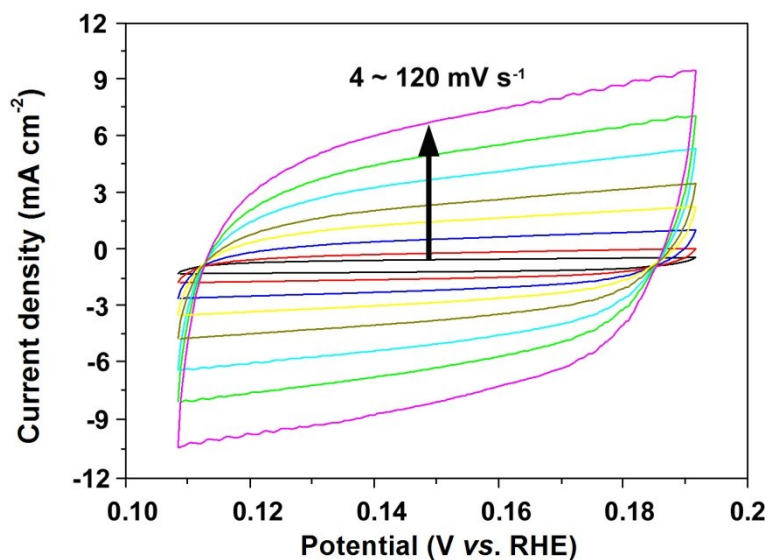


Fig. S6 Polarization curves of NiSP₃@G at potential from 0.108 V to 0.192 V vs RHE at scan rates of 4 mV/s, 10 mV/s, 20 mV/s, 40 mV/s, 60 mV/s, 80 mV/s, 80 mV/s, and 120 mV/s.

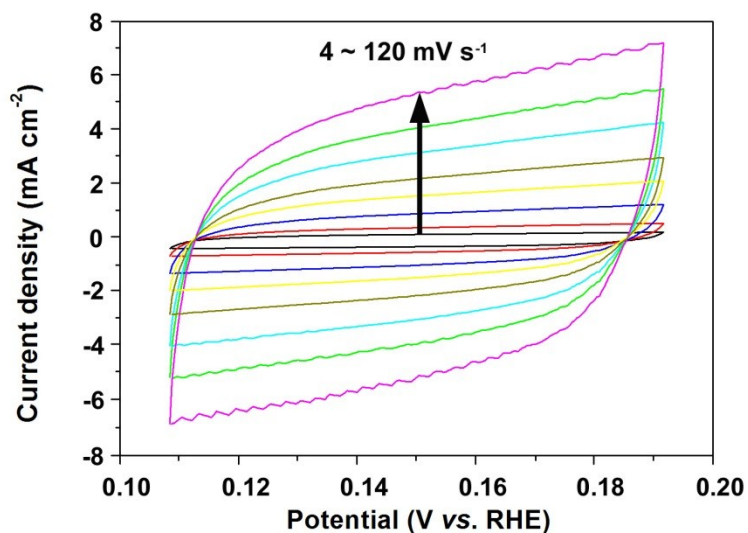


Fig. S7 Polarization curves of NiSP₃ at potential from 0.108 V to 0.192 V vs RHE at scan rates of 4 mV/s, 10 mV/s, 20 mV/s, 40 mV/s, 60 mV/s, 80 mV/s, 100 mV/s, and 120 mV/s.

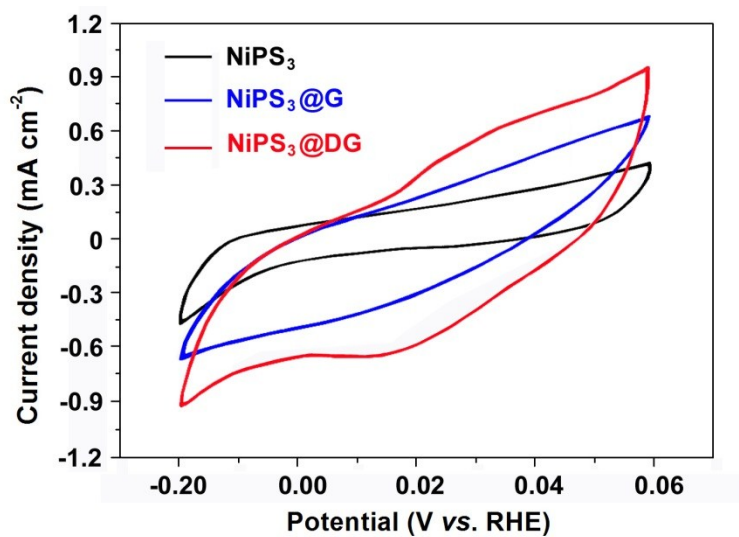


Fig. S8 CVs of the as-synthesized NiPS₃, NiPS₃@G, and NiPS₃@DG catalysts and bare GCE recorded at pH = 7 with a scan rate of 50 mV s⁻¹.

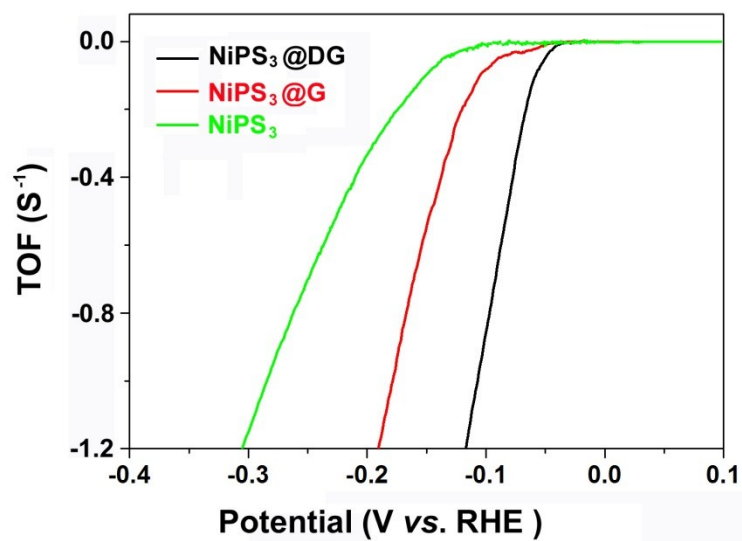


Fig. S9 Calculated TOFs for the as-synthesized catalysts in 0.5 M H_2SO_4 .

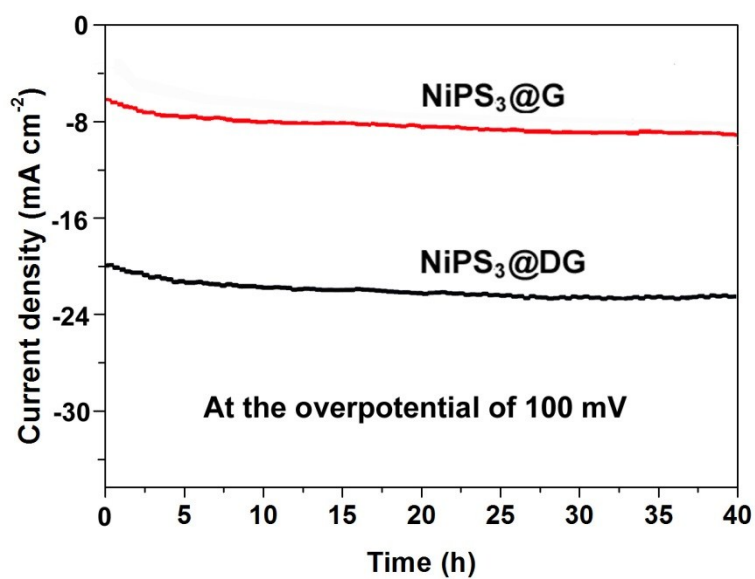


Fig. S10 Chronoamperometric curves of $\text{NiPS}_3@G$, and $\text{NiPS}_3@DG$ under static overpotential of 100 mV in 0.5 M H_2SO_4 .

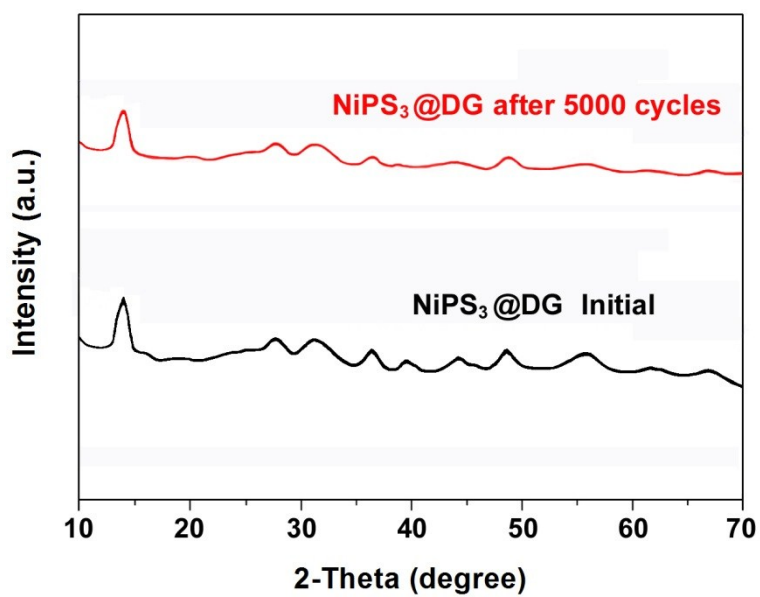


Fig. S11 XRD patterns of NiPS₃@DG before and after 5000 cycles.

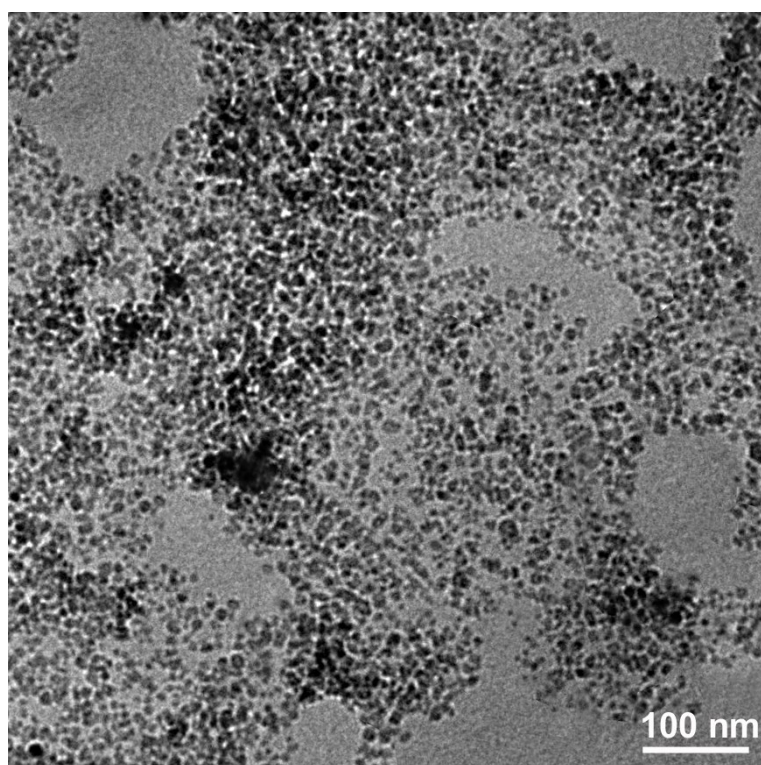


Fig. S12 TEM image of NiPS₃@G after 5000 cycles.

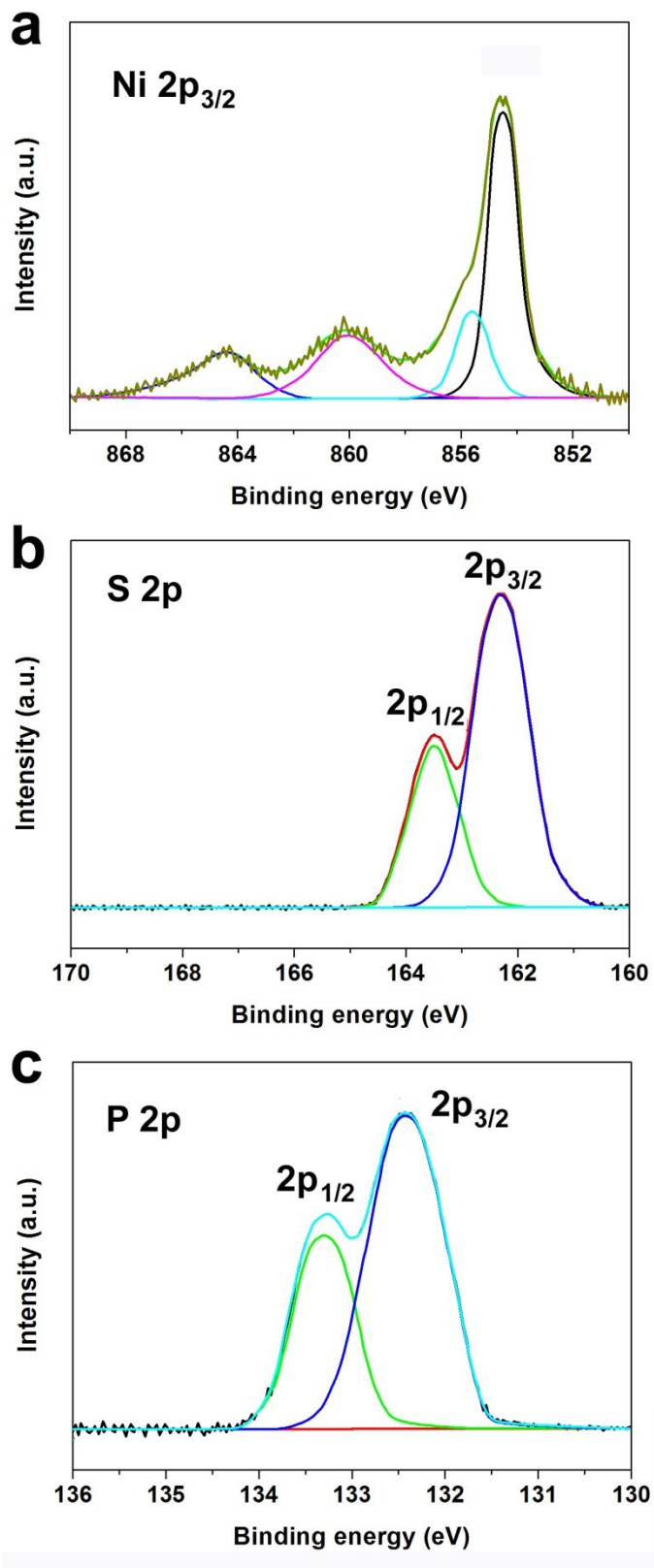


Fig S13 Core-level Ni 2p (a), S2p (b) and P2p XPS spectra of NiPS₃@DG after 5000 cycles.

Table S1 Comparison of the HER activity for several recently reported catalysts.

Catalysts	Catalyst amount (mg cm ⁻²)	Current density <i>j</i> (mA cm ⁻²)	Overpotentials (V vs. RHE) at the corresponding <i>j</i>	Reference
NiPS ₃ @DG	0.2	10	73	This work
NiPS ₃ @DG	0.2	20	98	This work
MnNi	0.28	10	360	Adv. Funct. Mater. 2015, 25, 393
CoO _x @CN	2.1	20	134	J. Am. Chem. Soc. 2015, 137, 2688.
CoFePO	2.2	10	87.5	ACS Nano 2016, 10, 8738
CoMnO@CN	2.0	10	~60	J. Am. Chem. Soc. 2015, 137, 14305
Ni@NC	0.35	10	190	Adv. Energy Mater. 2015, 5, 1401660
Ni _{2/3} Fe _{1/3} -GO	0.25	10	230	ACS Nano 2015, 9, 1977

CoP/rGO	0.28	10	150	Chem. Sci. 2016, 7, 1690
NiFeLDHNS@DG	0.28	10	300	Adv. Mater. 2017, 29, 1700017
Ni ₂ P/Ni/NF	-	10	98	ACS Catal. 2016, 6, 714
Mn-Co-P	5.61	10	81	ACS Catal. 2017, 7, 98– 102
CoP@BCN	0.4	10	87	Adv. Energy Mater. 2017, 1601671

References

- [1] Perdew, J. P.; Burke, K.; Ernzerhof, M. Generalized Gradient Approximation Made Simple. *Phys. Rev. Lett.* 1996, 77, 3865.
- [2] Kresse, G.; Furthmüller, J. Efficient Iterative Schemes for Ab Initio Total-Energy Calculations using a Plane-Wave Basis Set. *Phys. Rev. B* 1996, 54, 11169.
- [3] Kresse, G.; Joubert, D.; From Ultrasoft Pseudopotentials to the Projector Augmentedwave Method. *Phys. Rev. B* 1999, 59, 1758.

[4] Monkhorst, H. J.; Pack, J. D. Special Points for Brillouin-Zone Integrations. *Phys. Rev. B* 1976, 13, 5188.

[5] Merki, D.; Fierro, S.; Vrubel, H.; Hu, X. Amorphous Molybdenum Sulfide Films as Catalysts for Electrochemical Hydrogen Production in Water. *Chem. Sci.* 2011, 2, 1262–1267.